*Korean J. Chem. Eng.*, **16**(6), 778-783 (1999)

# Mathematical Model of a Monolith Catalytic Incinerator

**Soo Hyun Jang, Wha Seung Ahn†, Jae Mok Ha* and Kwang Ja Park***

School of Chemical Science and Engineering, Inha University, Inchon 402-751, Korea
*Agency for Technology and Standards, Kwacheon 427-010, Korea
*(Received 28 August 1999 • accepted 6 October 1999)*

**Abstract**–A set of 1-dimensional mathematical models were developed to simulate both the steady state and transient performance of monolithic catalytic incinerators for VOC abatement. In modelling transient performance, quasi-steady state gas phase was assumed since transient response time is determined primarily by the thermal inertia of the monolith. Higher inlet gas temperatures and lower gas velocities were predicted to give higher conversion and faster response times. VOC concentration had little influence on the performance within the concentration ranges used. A catalytic incinerator is shown to operate typically under mass transfer limited conditions, and monolith channel density and shape have significant influence on the conversion and monolith heating time. The metallic monolith was predicted to show superior steady state and transient responses due to its lower thermal inertia generated by higher cell density and thinner wall.

Key words: Catalytic Incinerator, Monolith, Mathematical Model, VOC

## INTRODUCTION

Volatile organic compounds (VOC's) are defined as organic compounds whose vapors may react photochemically in the atmosphere to form ozone or smog, and increasingly stringent regulations on their emission levels are being imposed. For effective removal of VOC's, a catalytic incinerator is increasingly used industrially due to its high VOC destruction efficiency and economic operation [Jennings et al., 1985].

For catalytic incinerators, catalytic units fabricated in a monolith type reactor are usually used because lower pressure drop and higher cross-section area to volume ratio proved to be advantageous over the packed bed type reactor [Heck and Farrauto, 1995]. Mathematical modeling of such devices was studied actively earlier with regard to its application to high temperature catalytic combustion [Stevens and Ziegler, 1977; Tien, 1981; Prasad et al., 1983] and still remains the subject of much interest [Jahn et al., 1997; Geus and Giezen, 1999]. The status of catalytic combustor models at various levels of sophistication have been reviewed by Trimm [1983] and more recently by Groppi et al. [1999]. Critical assessment of model assumptions employed in various models has also been reported [Hayes and Kolaczkowski, 1994; Kolaczkowski, 1999].

In this paper, a set of steady state and transient mathematical models for monolith catalytic incinerators are developed, and the effect of various operating conditions and monolith design parameters are examined using model simulation. It was attempted in this study to develop a simple 1 D model for catalytic combustors, easily tractable yet incorporating sufficient details of essential transport phenomena involved. The model governing equations based on fundamental physio-chemical principles are essentially identical to ones proposed earlier by others [Cerkanowicz et al., 1977; Votruba et al., 1975], but a new feature of estimating gas properties as a function of gas temperature in axial direction of the monolith was further implemented.

†To whom correspondence should be addressed.
E-mail: whasahn@dragon.inha.ac.kr

## MODEL DEVELOPMENT

### 1. Steady State Model

The following assumptions were made in developing a set of governing equations for a steady state catalytic incinerator model:

(1) The gas properties are uniform over the cross-section, but can be varied along the channel axis as a function of gas temperature (1 dimensional variable property model).

(2) The heterogeneous surface reaction is taken to be first order in hydrocarbon concentration and zero order in oxygen concentration under the air-excess operating conditions [Bennett et al., 1991; Groppi et al., 1995].

(3) The mass and heat transfer between the gas and solid phases are calculated using the transfer coefficients obtained from appropriate correlations for Nusselt and Sherwood numbers [Hawthorn, 1974].

$$Nu = A(1+0.095Re \cdot Pr \cdot d/L)^{0.45}$$

$$Sh = A(1+0.095Re \cdot Sc \cdot d/L)^{0.45}$$

(4) The gas velocity changes proportionally to the gas temperature (variable velocity model).

(5) Axial thermal radiation and conduction effects can be neglected.

Based on these assumptions, the material and energy balances for the gas and solid phase can be written as:

$$S\frac{d(VC_{fg})}{dX} = -\sigma k(C_{fg}-C_{fs}) \quad (1)$$

$$k(C_{fg}-C_{fs}) = Z_c \exp\left(-\frac{E_c}{RT_s}\right)C_{fs} \quad (2)$$

$$S\rho VC_p\frac{dT_g}{dX} = -\sigma h(T_g - T_s) \tag{3}$$

$$\sigma h(T_s - T_g) = \sigma(-\Delta H_c)Z_c\exp\left(-\frac{E_c}{RT_s}\right)C_{fs} \tag{4}$$

and continuity equation,

$$\frac{d}{dX}(\rho V) = 0 \tag{5}$$

Appropriate initial conditions are

$$C_{fg} = (C_{fg})_0,\ C_{O_2} = (C_{O_2})_0,\ V = V_0,\ T_g = T_0 \text{ at } x = 0 \tag{6}$$

By introducing dimensionless variables,

$$\zeta = \frac{X}{L},\ \Psi_{fs} = \frac{C_{fs}}{(C_{fg})_0},\ \nu = \frac{V}{V_0},\ \omega = \frac{V}{V_0}\cdot\frac{C_{fg}}{(C_{fg})_0} = \nu\cdot\Psi_{fg},$$
$$\theta_g = \frac{T_g}{T_0},\ \theta_s = \frac{T_s}{T_0} \tag{7}$$

and the dimensionless parameters,

$$J_D = \left(\frac{L}{V_0}\right)\left(\frac{\sigma k}{S}\right),\ J_H = \left(\frac{L}{V_0}\right)\left(\frac{\sigma h}{S\rho_g C_p}\right),\ D_c = \left(\frac{L}{V_0}\right)\left(\frac{\sigma Z_c e^{-\gamma}}{S}\right),$$
$$\Gamma = \frac{(C_{fg})_0(-\Delta H)}{\rho_0 C_p T_0},\ \gamma_c = \frac{E_c}{RT_0} \tag{8}$$

The governing Eqs. (1)-(4) can be written as

$$\frac{d\omega}{d\zeta} = -J_D\left(\frac{\omega}{\nu} - \Psi_{fs}\right) \tag{9}$$

$$J_D\left(\frac{\omega}{\nu} - \Psi_{fs}\right) = D_c\exp\left\{\frac{\gamma_c(\theta_s - 1)}{\theta_s}\right\}\Psi_{fs} \tag{10}$$

$$\frac{d\theta_g}{d\zeta} = J_H(\theta_s - \theta_g) \tag{11}$$

$$J_H(\theta_s - \theta_g) = \Gamma D_c\exp\left\{\frac{\gamma_c(\theta_s - 1)}{\theta_s}\right\}\Psi_{fs} \tag{12}$$

and initial conditions become

$$\Psi_{fg} = \nu = \omega = \theta_g = 1.0 \text{ at } \zeta = 0 \tag{13}$$

From (9), (10) and (12), it can be shown that (11) simplifies as

$$\frac{d\theta_g}{d\zeta} = -\Gamma\frac{d\omega}{d\zeta} \tag{14}$$

and, upon integration from 0 to $\zeta^*$, results

$$\theta_g = 1 + \Gamma(1 - \omega) \tag{15}$$

also, from (10) and (12), the variable $\theta_s$ can be written as

$$\theta_s = \theta_g + \Gamma\frac{J_D}{J_H}\left(\frac{\omega}{\nu} - \Psi_{fs}\right) \tag{16}$$

Finally, from (10), (15), and (16), the following relationship can be derived

$$f(\Psi_{fs}) = D_c\exp\left[\frac{\gamma_c\Gamma\left\{(1-\omega) + \frac{J_D}{J_H}\left(\frac{\omega}{\nu} - \Psi_{fs}\right)\right\}}{1 + \Gamma(1-\omega) + \Gamma\frac{J_D}{J_H}\left(\frac{\omega}{\nu} - \Psi_{fs}\right)}\right]\Psi_{fs} + J_D\Psi_{fs}$$
$$-J_D\frac{\omega}{\nu} = 0 \tag{17}$$

The steady state model development procedure is essentially identical to those adopted for other lumped parameter one-dimensional models by earlier researchers [Votruba et al., 1975; Stevens and Ziegler, 1977], and results in the set of governing equations that consist of a ordinary differential Eq. (9) with three algebraic Eqs. (15), (16), and (17). The computation cycle starts by solving Eq. (17) for $\Psi_{fs}$ using interval halving or Newton's method. After $\theta_g$ and $\theta_s$ in (15) and (16) are calculated, (9) is integrated to estimate $\omega$ using the simple Euler or Runge-Kutta 4th order method. These quantities are substituted back to Eq. (17) to start another cycle.

**2. Transient Model**

In developing a transient model, a quasi-steady gas phase in which accumulation of mass and energy in the gas phase is negligible was assumed because heat up/cooling down time for the catalytic solid phase is much larger than the gas residence time in catalytic combustor operation [Tien, 1981]. As a result of the quasi-steady state assumption, only the catalyst solid energy balance equation needs to be modeled as time-dependent as follows:

$$\sigma h(T_s - T_s) = \sigma(-\Delta H_c)Z_c\exp\left(-\frac{E_c}{RT_s}\right)C_{fs} - \rho_s C p_s S_s\frac{\partial T_s}{\partial t} \tag{18}$$

with boundary and initial conditions:

$$C_{fg}(0, t) = (C_{fg})_0,\ T_g(0, t) = (T_g)_0,\ T_s(x, 0) = \text{specified}(T_s)_0,$$
$$C_{fs}(x, 0) = (C_{fg})_0,\ V(0, t) = V_0 \tag{19}$$

By introducing dimensionless parameter $\alpha = \frac{(\rho Cp)_s}{(\rho Cp)_0}\left(\frac{S_s}{S}\right)\left(\frac{L}{V_0 t_0}\right)$, and dimensionless variable $\tau = \frac{t}{t_0}$, (18) and (19) can be written as

$$J_H(\theta_s - \theta_g) = \Gamma D_c\exp\left\{\frac{\gamma_c(\theta_s - 1)}{\theta_s}\right\}\Psi_{fs} - \alpha\frac{\partial\theta_s}{\partial\tau} \tag{20}$$

$$\omega(0, \tau) = \theta_g(0, \tau) = \nu(0, \tau) = 1.0,\ \theta_s(\zeta, 0) = \text{specified } ((\theta_s)_0),$$
$$\Psi_{fs}(\zeta, 0) = 1.0 \tag{21}$$

New, the set of Eqs. (9), (10), (11) and (20) make up the transient model for the catalytic incinerator. Computation starts by solving (9) and (11) for $\omega$ and $\theta_g$ by Euler method using the initial values of the solid surface concentration and solid temperature in (21). Then $\theta_s$ at next time step is estimated by approximating (20) by

$$\theta_{s\,x}^{\ t} = \frac{\Delta t}{\alpha}\left[-J_H\{\theta_{s\,x}^{\ t-1} - \theta_{g\,x}^{\ t-1}\} + \Gamma D_c\exp\left\{\frac{\gamma_c(\theta_{s\,x}^{\ t-1} - 1)}{\theta_{s\,x}^{\ t-1}}\right\}\right.$$
$$\left.\Psi_{fs\,x}^{\ t-1}\right] + \theta_{s\,x}^{\ t-1} \tag{22}$$

Subsequently, (10) is solved by interval halving method to find $\Psi_{fs}$. These iterative computations are continued until computed catalyst surface temperatures show less than 0.001% difference in two successive iterations.

## RESULTS AND DISCUSSION

The catalytic incinerator simulation was conducted by using

**Table 1. Standard inlet conditions**

| | | | |
|---|---|---|---|
| T=523.15 °K, | V=250 cm/s, | P=1 atm, | $C_{MIBK}$=0.2% |

methyl isobutyl ketone (MIBK) as a representative VOC. The kinetic parameters used in this study are $E_c$=11.2 Kcal/mol and $Z_c$=0.05 (cm/sec)·(mol/cm$^3$) for Pd/$Al_2O_3$ catalyst [Kim and Ahn, 1995]. The standard set of inlet conditions adopted for this study is listed in Table 1, and typical dimensions and physical properties of monoliths are summarized in Table 2. Unless otherwise stated, a ceramic monolith with 31 cells/cm$^2$ was assumed as a standard support.

Fig. 1 and Fig. 2 show the transient development of the gas temperature ($\theta_g$) and the solid temperature ($\theta_s$) profiles when a monolith initially at room temperature is subjected to a step change in input conditions corresponding to values in Table 1. Fig. 3 shows the concurrent changes in gas conversion profile with time. At early times of warm-up (t=5 sec), the hot gas stream heats up the entire monolith by convective heat transfer. As time elapses (t=10 sec), the heat generated by catalytic reaction raises the solid temperature above the gas temperature at the front section of the monolith and hence the gas stream is now being heated by the hotter solid. The gas stream arrives at the

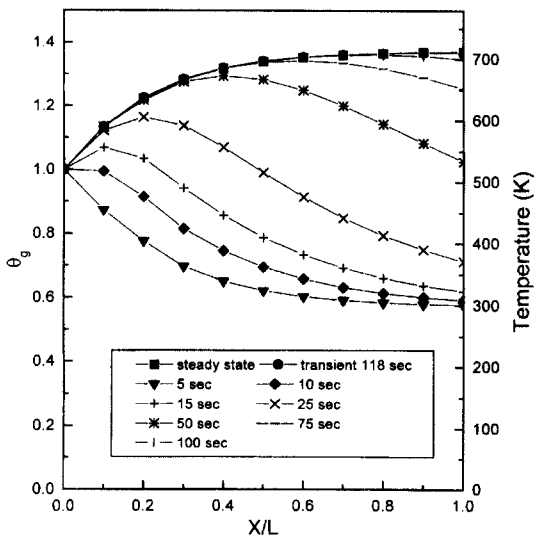


**Fig. 1. Transient gas temperature profiles.**

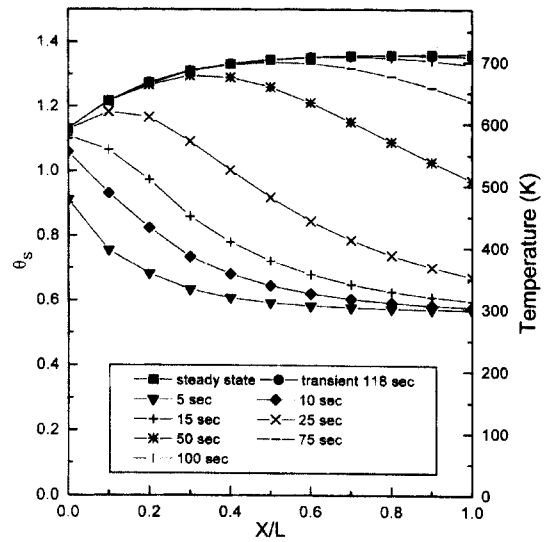


**Fig. 2. Transient solid temperature profiles.**

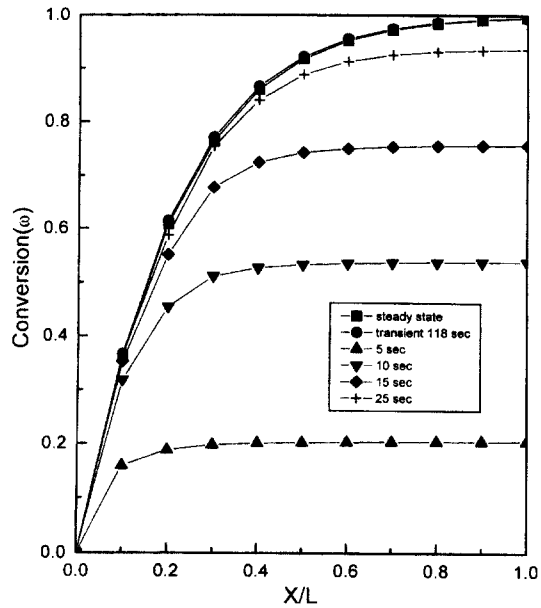


**Fig. 3. Transient gas conversion profiles.**

downstream section at high temperatures as a result of heating by the hotter solid in the upstream section, and consequently

**Table 2. Physical properties of monolith [Cooper et al., 1978]**

| Properties | Ceramic | | | Metallic |
|---|---|---|---|---|
| Cell type | 31 cells/cm$^2$ | 46.5 cells/cm$^2$ | 93 cells/cm$^2$ | 62 cells/cm$^2$ |
| Length (cm) | | 10 | | |
| d (cm) | 0.154 | 0.1212 | 0.0738 | 0.12 |
| A | square | triangle | | circle |
| | 2.98 | 2.35 | | 3.66 |
| σ (cm) | 0.616 | 0.485 | 0.313 | 0.54 |
| S (cm$^2$) | 0.0238 | 0.0147 | 0.0061 | 0.015 |
| Solid cross sectional area (cm$^3$) | 0.0085 | 0.0068 | 0.0046 | 0.011 |
| Solid density (g/cm$^3$) | | 2.5 | | 7.76 |
| Heat capacity [cal/(g·K)] | | 0.219 | | 0.11 |

the gas temperatures near the monolith exit are higher than the solid temperatures. MIBK conversion increases monotonically from the entrance to the exit of the incinerator, and reaches over 95 percent at 25 sec. This process of the hotter gas stream heating the solid in the downstream section of monolith is maintained until the system attains a new steady state at t=118 sec, where the exit solid temperature is slightly higher than the gas temperature, and MIBK conversion reaches about 99.5 percent.

Having established the behaviour of the monolith for standard conditions, we studied the effect of changing operating conditions on monolith performance by varying inlet gas temperature, VOC concentration, and velocity in turn while keeping the rest of the operating variables constant to the standard conditions in Table 1. Fig. 4 shows a plot of computed steady state exit conversions as a function of inlet gas temperature at standard operating conditions. Increasing the inlet gas temperature shows that the catalyst lights-off at ca. 373 K, and the exit conversion increases sharply immediately after it. Inlet temperature of approximately 398 K is necessary to achieve conversion in excess of 95 percent. The conversion after ignition, however, is limited by mass transfer rate of chemical species to the catalyst surface, and further increases in gas inlet temperature have little effect on the exit conversion. Fig. 5 shows the exit conversion as a function of MIBK concentration. Computations were performed over the concentration between 200 and 4,000 ppm, which was reported to be the concentration range usually encountered in practice [Heck and Farrauto, 1995]. Exit conversion higher than 98.5% was predicted over the concentration range, which tends to rise monotonically with increasing VOC concentration due to the higher amount of heat generated with increasing VOC concentrations. This feature explains why a concentrating device such as an adsorption bed is desirable in conjunction with a catalytic combustor for treatment of VOC with low concentration to achieve higher combustion efficiency. Fig. 6 shows the effect of inlet gas velocity on exit conversions. Corresponding dimensionless parameters for heterogeneous reaction rate ($D_C$) and heat and mass transfer processes ($J_H$, $J_D$) are also plotted. For simplicity, the parameter values evaluated at inlet gas temperature were shown. Increases in inlet gas velocity are accompanied by reduction in gas residence time within the monolith ($L/V_0$) and increases in heat (Nu) and mass (Sh) transfer coefficients. Under the operating conditions simulated, Reynolds numbers obtained were all below 2,000, i.e., laminar flow condition prevails, and reduction in gas residence time has a dominant effect over the heat/mass transfer rate increases on the catalytic monolith reactor. The catalytic Damkohler number, $D_C$, represents gas residence time ($L/V_0$) over catalytic reaction time such that increasing velocity at fixed inlet temperature causes a linear decrease in $D_C$. In our model, heat and mass transfer rates are reflected in changes in the dimensionless coefficients, $J_H$ and $J_D$, which represent the

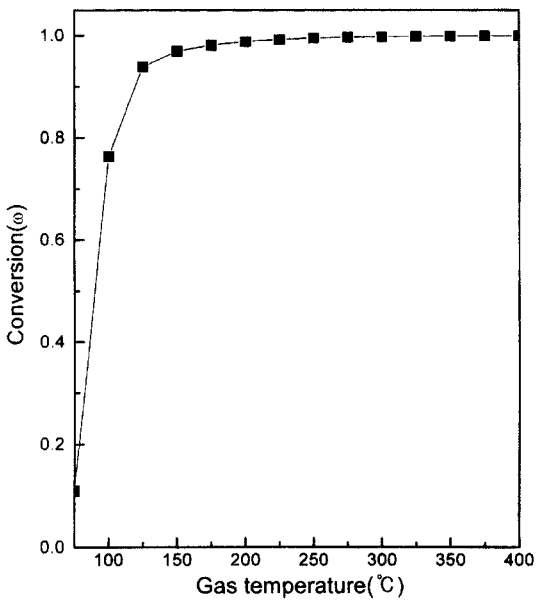


**Fig. 4. Effect of gas inlet temperature on exit conversion.**

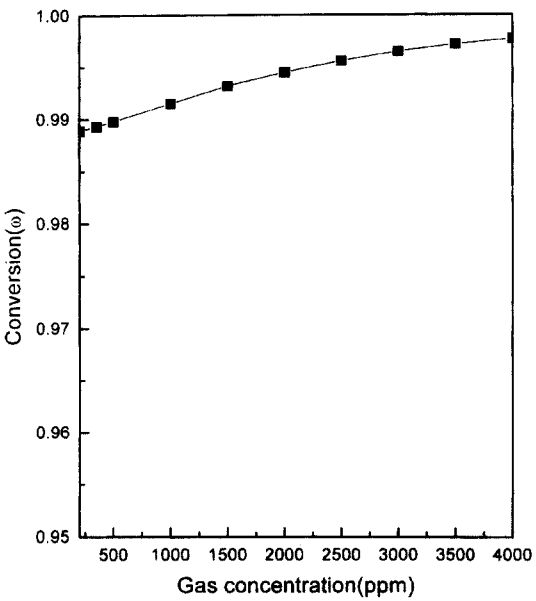


**Fig. 5. Effect of gas inlet concentration on exit conversion.**

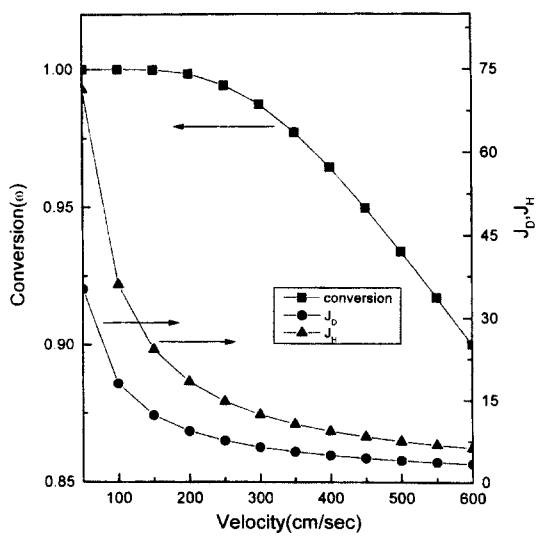


**Fig. 6. Effect of gas velocity on exit conversion.**

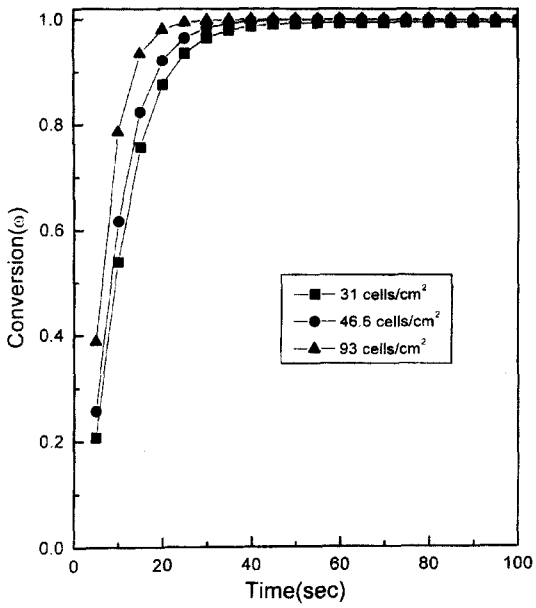


**Fig. 7. Effect of channel density on exit conversion as a function of time.**

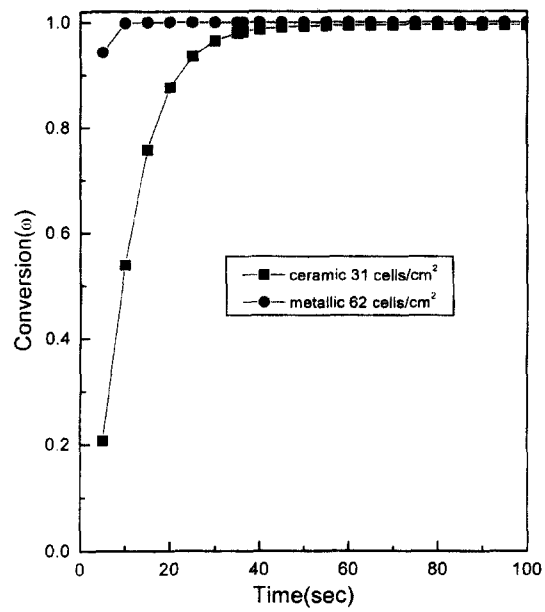


**Fig. 8. Effect of monolith type on exit conversion as a function of time.**

ratio of gas residence time in the reactor to heat and mass transfer time, respectively. As gas inlet velocity increases from 50 cm/sec to 600 cm/sec, $J_H$ and $J_D$ decrease continuously due to dominant reduction in gas residence time and hence exit conversion decreases monotonically as gas velocity increases.

Metallic or ceramic monoliths may be applied in a catalytic combustor, and the properties and design of monoliths can have important bearing on the performance of the reactor. Fig. 7 compares the effect of monolith channel density on conversion in time domain. As the cell density increases, higher surface to volume ratio of the monolith is achieved, making more efficient contact with the gas phase, and the cross-sectional area of an individual cell decreases, improving mass transport of reactants to the reactor wall. As a consequence, increasing cell density from 31 to 93 cells/cm$^2$ improves catalytic incinerator performance. Fig. 8 compares the performance of a 62 cells/cm$^2$ metallic monolith with the standard 31 cells/cm$^2$ ceramic monolith. The metallic monolith, due to its extremely thin wall thickness, has higher cell density and much smaller thermal inertia than the ceramic monolith. As a result, the metallic monolith shows much faster attainment of steady state (t=32 sec) compared with the ceramic monolith (t=118 sec). Fig. 9 illustrates the influence of channel geometry on conversion of VOC in catalytic monoliths. The value of the asymptotic Nusselt number (Nu) for laminar flow in ducts varies depending on the duct shape such that higher Nu is obtained in the order of circular>square>triangular shaped channels. Higher mass transfer rates (Sh) are also achieved in the same order in shape as for the heat transfer rates. According to the computational results, a monolith having circular channels achieves the earliest steady state (t=113 sec<t=118 sec square<t=125 sec triangular). This is because the circular channelled monolith, which has the highest Nu among the three monoliths is heated by the gas phase more rapidly than the others. Steady state performance also follows the same order, since a circular shaped cell

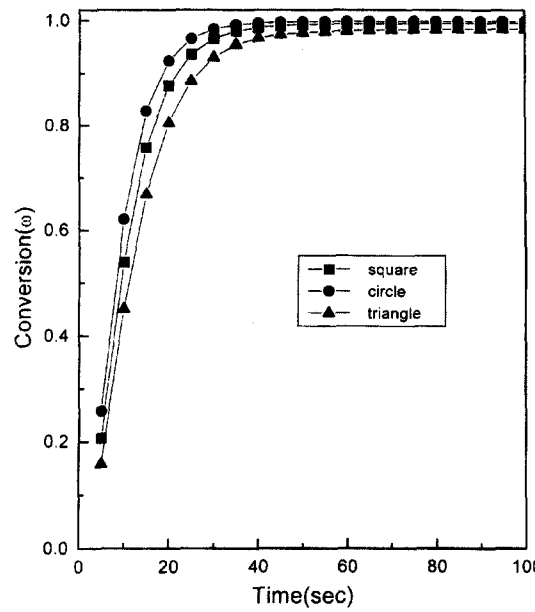


**Fig. 9. Effect of channel shape on exit conversion as a function of time.**

would be advantageous due to enhanced mass transfer rates provided under the typically mass transfer limited reaction conditions after catalyst light-off.

## CONCLUSIONS

A simple set of mathematical models for monolith catalytic incinerators for MIBK were proposed by considering first order heterogeneous reaction at the catalyst surface and variable gas properties and heat/mass transfer rates in axial direction. For transient behaviour, a quasi-steady state gas phase was as-

sumed. This study established that:

1. Under typical operating conditions, the incineration system is controlled by the mass transport rates of reactants from bulk gas stream to catalytic solid surface.

2. Catalytic incinerator performance is strongly dependent on inlet gas temperature and velocity. Catalyst light-off is achieved at approximately 373 K and the conversion below the light-off is kinetically controlled and very low, while the process is mass transfer-limited after ignition. Increasing inlet gas velocity in laminar flow regime decreased gas residence time in monolith channel such that conversion decreased monotonically upon its increase. The concentration has relatively little effect on conversion and conversion is shown over 95 percent under the typical concentration range of VOC emissions.

3. Increasing cell density improves catalytic incinerator performance, and metallic monoliths having higher cell density and smaller thermal inertia are superior to that of the ceramic monolith. Circular cell monoliths were predicted to perform better than square or triangular cell monoliths due to enhanced heat and mass transfer rates achieved.

## NOMENCLATURE

A : shape factor
$C_{fg}$ : gas phase fuel concentration [gmol/cm$^3$]
$C_{fs}$ : solid phase fuel concentration [gmol/cm$^3$]
$C_p$ : specific heat capacity [cal/g·K]
$D_c$ : catalytic Damkohler number
$E_c$ : catalytic activation energy [cal/gmol]
h : heat transfer coefficient [cal/sec·cm$^2$·K]
$J_D$ : mass transport number
$J_H$ : heat transfer number
k : mass transfer coefficient [cm/sec]
Nu : Nussult number
P : pressure [atm]
Pr : Prandtl number
Re : Reynolds number
S : channel cross-section area [cm$^2$]
Sc : Schmidt number
Sh : Sherwood number
$S_s$ : solid cross-section area [cm$^2$]
$T_s$ : solid temperature [K]
V : linear velocity [cm/sec]
X : axial distance [cm]
$Z_c$ : catalytic pre-exponential factor [cm/sec·gmol/cm$^3$]

### Greek Letters

$\alpha$ : thermal capacity ratio
$\gamma_c$ : dimensionless catalytic activation energy
$\Gamma$ : dimensionless adiabatic flame temperature
$\zeta$ : dimensionless axial distance
$\theta_g$ : dimensionless gas temperature
$\theta_s$ : dimensionless solid temperature
$\nu$ : dimensionless velocity
$\rho$ : density [g/cm$^3$]
$\sigma$ : wetted perimeter [cm]
$\tau$ : dimensionless time
$\Psi_{fs}$ : dimensionless solid phase concentration
$\omega$ : dimensionless mass fraction

## REFERENCES


Bennett, C. J., Kolaczkowski, S. T. and Thomas, W. J., "Determination of Heterogeneous Reaction Kinetics Rates Under Mass Transfer Controlled Conditions for a Monolith Reactor," *Trans. Instn. Chem. Engrs.*, **69**, Part B, 209 (1991).

Cerkanowicz, A. E., Cole, R. B. and Stevens, J. G., "Catalytic Combustion Modelling: Comparisons with Experimental Data," *Trans. ASME, Ser. A. J. Engng Power*, **99**, 593 (1977).

Cooper, B. J. and Strom, T., Rolles Royce Ltd., Aero-division Project Report No. 197 (1978).

Geus, J. W. and van Giezen, J. C., "Monoliths in Catalytic Oxidation," *Catalysis Today*, **47**, 169 (1999).

Groppi, G., Belloli, A., Tronconi, E. and Forzatti, P., "Analysis of Multidimensional Models of Monolith Catalysts for Hybrid Combustors," *AIChE Journal*, **41**, 2250 (1995).

Groppi, G., Tronconi, E. and Forzatti, P., "Mathematical Models of Catalytic Combustors," *Catal. Rev. Sci. Eng.*, **41**, 227 (1999).

Hawthorn, R. D., "Afterburner Catalysts-Effects of Heat and Mass Transfer Between Gas and Catalyst Surface," *AIChE Symp. Ser.*, **70**, 428 (1974).

Hayes, R. E. and Kolaczkowski, S. T., "Mass and Heat Transfer Effects in Catalytic Monolith Reactors," *Chem. Eng. Sci.*, **49**, 3587 (1994).

Heck, R. M. and Farrauto, R. J., "Catalytic Air Pollution Control," Van Nostrand Reinhold (1995).

Jahn, R., Snita, D., Kubicek, M. and Marek, M., "3-D Modelling of Monolith Reactors," *Catalysis Today*, **38**, 39 (1997).

Jennings, M. S., Krohn, N. E., Berry, R. S., Palazzolo, M. A., Parks, R. M. and Fidler, K. K., "Catalytic Incineration for Control of Volatile Organic Compound Emissions," Park Ridge, N. J. (1985).

Kim, J. S. and Ahn, W. S., "A Study on the Catalytic Incineration of Methyl Isobutyl Ketone," *J. of Korean Ind. & Eng. Chemistry*, **6**(4), 690 (1995).

Kolaczkowski, Stan T., "Modelling Catalytic Combustion in Monolith Reactors-Challenges Faced," *Catalysis Today*, **47**, 209 (1999).

Prasad, R., Kennedy, L. and Ruckenstein, E., "A Model for the Transient Behavior of Catalytic Combustors," *Comb. Sci. Tech.*, **30**, 59 (1983).

Stevens, J. G. and Ziegler, E. N., "Effect of Momentum Transport on Conversion in Adiabatic Catalytic Tubular Reactors," *Chem. Eng. Sci.*, **32**, 385 (1977).

Tien, J. S., "Transient Catalytic Combustor Model," *Comb. Sci. Tech.*, **26**, 65 (1981).

Trimm, D., "Catalytic Combustion," *Appl. Catal.*, **7**, 249 (1983).

Votruba, J., Sinkule, J., Hlavacek, V. and Skrivanek, J., "Heat and Mass Transfer in Monolithic Honeycomb Catalysts-I," *Chem. Eng. Sci.*, **30**, 117 (1975).